© 2016. Published by The Company of Biologists Ltd | Journal of Cell Science (2016) 129, 2462-2471 doi:10.1242/jcs.184523

TOOLS AND TECHNIQUES

An optical method to evaluate both mass and functional competence of pancreatic α- and β-cells

Yi Wang[1,2], Chengsheng Han[2], Wenzhen Zhu[2], Zhengxing Wu[1], Yanmei Liu[2,*] and Liangyi Chen[2,*]

ABSTRACT

Imbalanced glucagon and insulin release leads to the onset of type 2 diabetes. To pinpoint the underlying primary driving force, here we have developed a fast, non-biased optical method to measure ratios of pancreatic α- and β-cell mass and function simultaneously. We firstly label both primary α- and β-cells with the red fluorescent probe ZinRhodaLactam-1 (ZRL1), and then highlight α-cells by selectively quenching the ZRL1 signal from β-cells. Based on the signals before and after quenching, we calculate the ratio of the α-cell to β-cell mass within live islets, which we found matched the results from immunohistochemistry. From the same islets, glucagon and insulin release capability can be concomitantly measured. Thus, we were able to measure the ratio of α-cell to β-cell mass and their function in wild-type and diabetic $Lepr^{db}$/$Lepr^{db}$ (denoted *db*/*db*) mice at different ages. We find that the initial glucose intolerance that appears in 10-week-old *db*/*db* mice is associated with further expansion of α-cell mass prior to deterioration in functional β-cell mass. Our method is extendable to studies of islet mass and function in other type 2 diabetes animal models, which shall benefit mechanistic studies of imbalanced hormone secretion during type 2 diabetes progression.

KEY WORDS: Insulin secretion, Glucagon secretion, Diabetes, α-cell mass, β-cell mass, Islets

INTRODUCTION

The blood glucose level is tightly regulated under normal conditions, and its dysregulation leads to diabetes mellitus, which affects millions of people. Pancreatic β-cells secrete insulin to activate the glucose uptake of cells such as adipocytes and muscle cells, whereas α-cells secrete glucagon to stimulate glucose synthesis from the liver through the hydrolysis of glycogen and gluconeogenesis. Many researchers studying diabetes hold the view that a decrease in functional β-cell mass, which manifests as either a decrease in the β-cell number or a reduction in the β-cell secretory ability, is a primary factor that leads to hyperglycemia (Weir and Bonner-Weir, 2004). Increases in α-cell mass and glucagon hypersecretion during the pathogenesis of type 2 diabetes have also been reported (Unger and Cherrington, 2012). However, α-cell dysregulation is often regarded as secondary to either impaired β-cell mass or reduced insulin secretion; therefore, the roles of α-cells during type 2 diabetes are usually overlooked (D'Alessio, 2011; Quesada et al., 2008). In contrast to this dogma, specific microRNAs and cytokines that maintain only α-cell mass but not β-cell mass are found to be upregulated in obesity and type 2 diabetes (Ellingsgaard et al., 2008; Guardado-Mendoza et al., 2013; Poy et al., 2009). Moreover, in rats that are chronically infused with glucose for 10 days, hyperglucagonemia precedes a decline in the insulin secretion, which causes hyperglycemia (Jamison et al., 2011). Therefore, the upregulation of glucagon secretion and α-cell mass during the progression of type 2 diabetes could contribute to hyperglycemia, independently of changes in β-cell mass and function. Regarding the masses and functions of α- and β-cells, the primary driving force for the imbalanced glucagon and insulin secretion at different stages of type 2 diabetes progression is still unknown and is a pending question in the field.

To address such a question, a systematic examination of α- and β-cell masses and functions at different disease stages is needed. The 'functional β-cell mass' calculated by measuring blood glucose and insulin levels in human patients (Cobelli et al., 2007) does not differentiate impaired β-cell mass from declining function. Immunohistochemistry (IHC) is the gold standard for quantifying α- and β-cell masses within fixed pancreas slices. However, the corresponding cellular function within fixed samples cannot be measured in concert with this technique. Moreover, because of the reciprocal regulations between hormone secretion and the circulating blood glucose level, it is difficult to determine the causal relationship by *in vivo* measurements. Islet hormone secretion is also modulated by neurotransmitters that are locally released from intra-islet nerve terminals (Koh et al., 2012), circulating nutrients other than glucose in blood vessels (Nolan et al., 2006) and incretins that are released from intestinal cells (Campbell and Drucker, 2013), which are all subjected to alteration during type 2 diabetes progression. Therefore, mechanistic studies require live islets or cells to be isolated and their functions to be measured *in vitro* independently of environmental factors. However, isolated α-cells are more difficult to study than β-cells, which could contribute to the fact that the number of research papers on glucagon is one-tenth that for insulin in a Medline search (Henquin et al., 2011). A major hurdle in this field is to identify the sparse α-cells from the abundant β-cells within live islets. Although transgenic mouse islets with fluorescently labeled α-cells are available (Quoix et al., 2007), they are not widely used. Thus, a simple and fast method is needed to separate α-cells from β-cells to study their masses and functions in different animal models.

Here, we develop a new method to differentiate α-cells from β-cells in islets taking advantage of the red fluorescent probe ZinRhodaLactam-1 (ZRL1) (Du and Lippard, 2010), which contains a rhodamine B nonfluorescent lactam form and a Zn^{2+}-binding ligand (Fig. 1A). We found that ZRL1 labels both α-cells and β-cells at a similar intensity. However, application of *N*,*N*,*N*′,*N*′-tetrakis-(2-pyridylmethyl)ethylenediamine (TPEN), a Zn^{2+} chelator, effectively quenched the fluorescence from the β-cells but left the fluorescence from the α-cells intact. This enables

[1]College of Life Science and Technology, Huazhong University of Science and Technology, Wuhan 430074, China. [2]State Key Laboratory of Membrane Biology, Beijing Key Laboratory of Cardiometabolic Molecular Medicine, Institute of Molecular Medicine, Peking University, Beijing 100871, China.

*Authors for correspondence (lychen@pku.edu.cn; yanmeiliu@pku.edu.cn)

Y.W., 0000-0001-7956-3102; L.C., 0000-0003-1270-7321

Received 9 December 2015; Accepted 28 April 2016

Journal of Cell Science

Journal of Cell Science (2016) 129, 2462-2471 doi:10.1242/jcs.184523

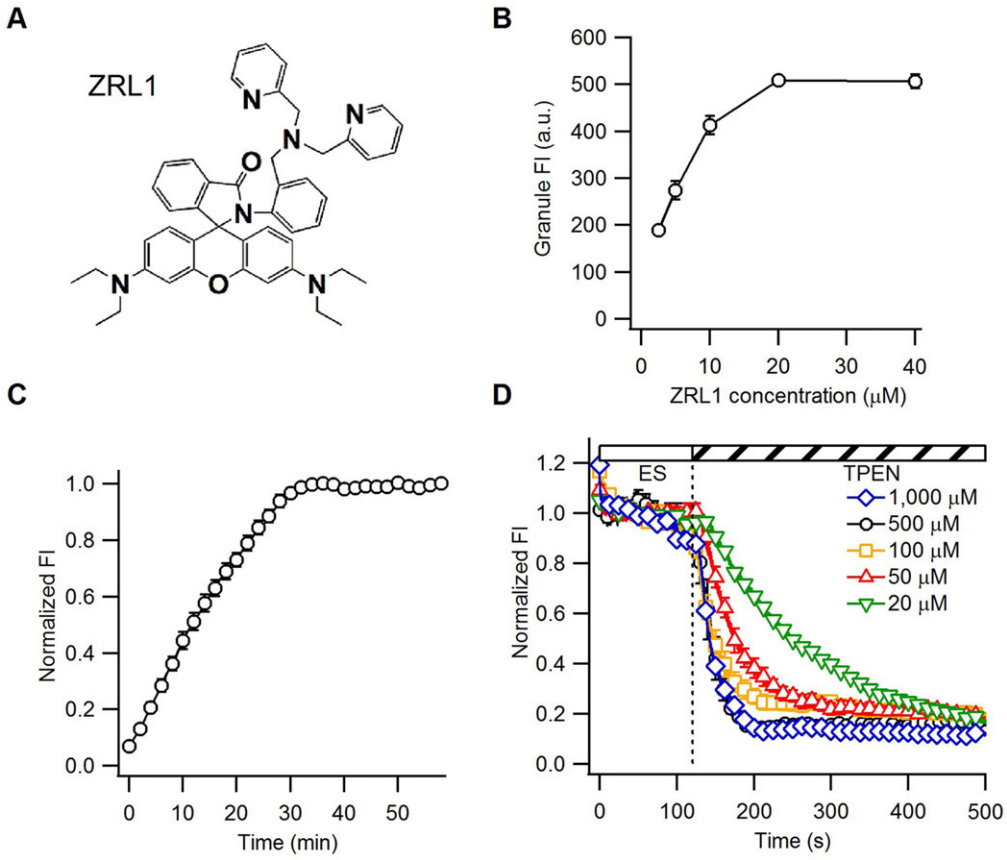

Fig. 1. Optimization of the ZRL1-TPEN loading protocol. (A) Chemical formula of ZRL1. (B) ZRL1 fluorescence intensity of granules from dispersed cells loaded with different ZRL1 concentrations for 40 min. Because granular intensity at the 20 μM ZRL1 loading condition was already saturated, we chose that concentration for all the other experiments. Results are mean±s.e.m. (*n*=1000). a.u., arbitrary units. (C) ZRL1 fluorescence dynamics in islet cells upon 20 μM ZRL1 loading. The fluorescence signal was acquired at a 1-min time interval as soon as dye was added and was normalized to the maximal platform fluorescence of the cell. The plot is the mean±s.e.m. result from 20 cells. (D) Timecourses of the fluorescent intensity of ZRL1-labeled granules in primary β-cells during treatment with different concentrations of TPEN. Fluorescence was normalized to the basal level. Results are mean±s.e.m. (*n*=6). ES, extracellular solution.

identification of pancreatic α-cells from islets for functional study. Based on this property, we also established a fluorescence quenching assay (FQA) to rapidly measure ratio of the α-cell to β-cell mass in live islets, which matched that acquired using the IHC method from pancreas slices in multiple experimental trials. Moreover, by measuring insulin and glucagon release from the same islets subjected to the FQA, a comparison of both mass and functional competence of α- and β-cells in live islets became possible. By examining the islets from wild-type and diabetic *Lepr*^{db}/*Lepr*^{db} (denoted *db/db*) mice at different stages, we reveal that increases in both the functional ratio and mass ratio of α/β cells are correlated with the deterioration of glucose tolerance. The increase in the functional ratio was less than that of the mass ratio of α- and β-cells in ten-week-old *db/db* islets, which suggests a primary role of α-cell mass expansion in disrupting the glucose tolerance at this early stage of type 2 diabetes.

RESULTS

Distinguishing α-cells from β-cells by ZRL1 labeling followed by TPEN quenching

ZRL1 is a non-fluorescent molecule that can cross cell membranes and emit red fluorescence upon binding to Zn^{2+} (Fig. 1A). Compared to other Zn^{2+} sensors, ZRL1 exhibits a relatively low affinity for Zn^{2+} (Du and Lippard, 2010). Considering the high concentration of Zn^{2+} inside insulin granules (Li, 2014), we assumed that the loading of islet cells with ZRL1 would selectively result in fluorescence accumulation in β-cells only. After optimizing the loading time and dye concentration to ensure maximum cellular fluorescence (Fig. 1B,C; see Materials and Methods), we found fluorescent puncta in all of the dissociated islet cells (Fig. S1A). To dissect the possible difference in the ZRL1 labeling between the β- and α-cells, we applied ZRL1 to the islet cells from GluCre-ROSA26EYFP (GYY) mice, in which α-cells are specifically labeled with EYFP (Fig. 2A). EYFP-positive α-cells and EYFP-negative non-α-cells displayed similar fluorescence intensities (Fig. 2C). Extracellular application of TPEN, a small membrane-permeable chemical that exhibits 10^{11} times greater affinity for Zn^{2+} than ZRL1 (Colvin et al., 2008), almost completely quenched ZRL1 fluorescence in non-α-cells within ∼100 s (quenching coefficient, 16±1% of the control, mean±s.e.m., *n*=9, Fig. 1D), but only marginally affected the fluorescence in EYFP-positive α-cells (quenching coefficient, 79±2% of the control, *n*=11, Fig. 2A,B; Movie 1). ZRL1 puncta in EYFP-negative non-α-cells colocalized with FFN511, a false fluorescent neurotransmitter that accumulates in dense-core vesicles, and FFN511 also colocalized with immunostained insulin in fixed β-cells (Fig. S1B). Therefore, the TPEN-quenchable fluorescence puncta in β-cells were indeed insulin granules. In contrast, the TPEN-resistant ZRL1 fluorescence in α-cells was rapidly eliminated after the perfusion of NH_4Cl (<10 s) (Fig. 2D; Movie 1), which neutralizes the intravesicular acidic pH, in agreement with the turn on of ZRL1 fluorescence at acidic pH in absence of Zn^{2+} (Du and Lippard, 2010). Under a spinning disc confocal microscope, ∼1817±118 ZRL1-labeled puncta (*n*=15, detailed in Materials and Methods) were identified in a single α-cell, most likely corresponding to acidic glucagon-containing granules.

We further proved the identity of TPEN-quenchable cells by immunofluorescence staining. After imaging the TPEN-quenched ZRL1 fluorescence of the dissociated islet cells, we fixed cells and labeled them with either anti-insulin plus anti-glucagon antibodies or anti-somatostatin antibody. A total of 95% of the TPEN-quenchable cells were β-cells (35 out of 37 cells; Fig. 2E), only 5%

Journal of Cell Science

Journal of Cell Science (2016) 129, 2462-2471 doi:10.1242/jcs.184523

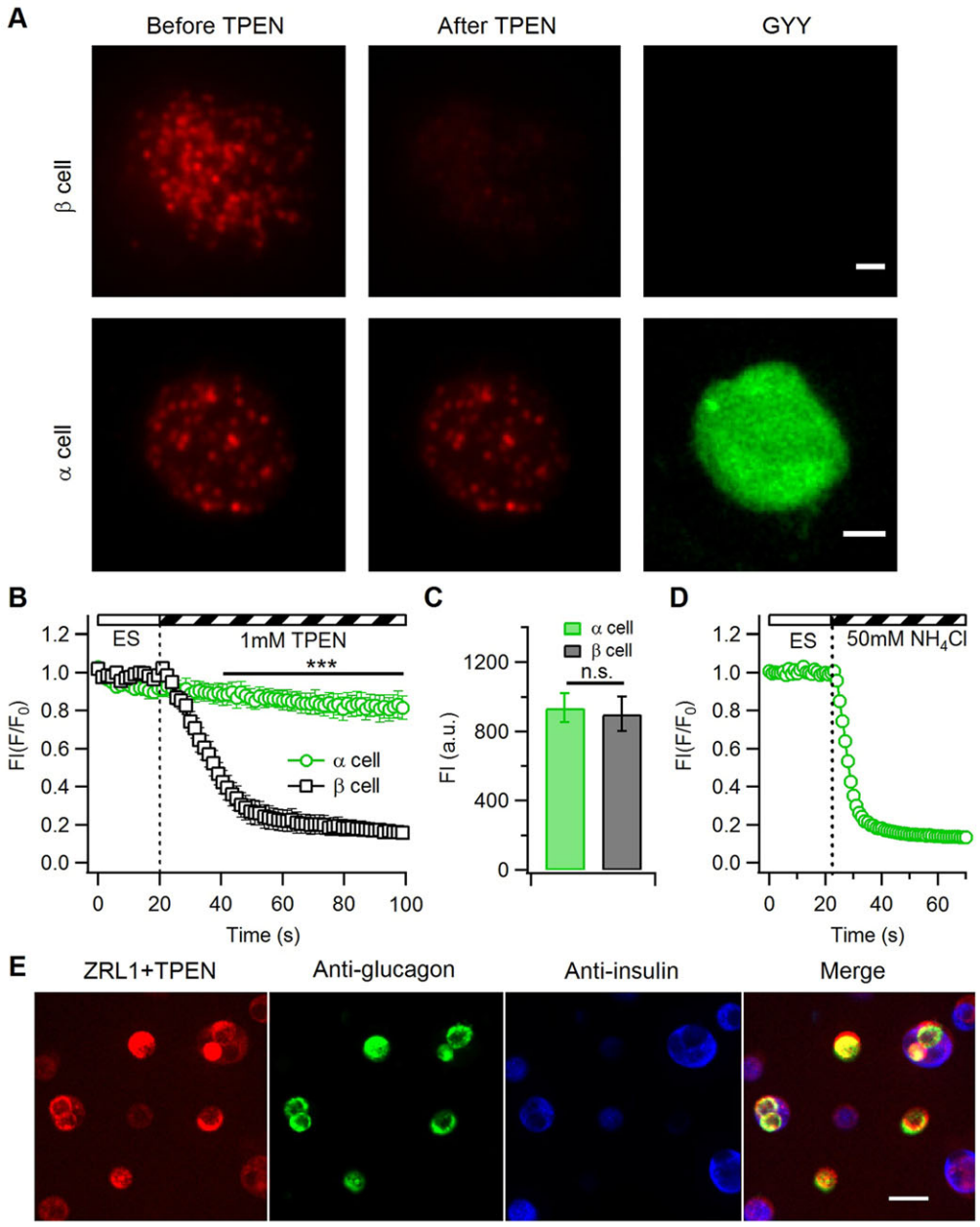

Fig. 2. ZRL1 fluorescence is susceptible to TPEN quenching in primary β-cells but not in α-cells. (A) Representative examples of a ZRL1-labeled EYFP-negative β-cell (top), and a ZRL1-labeled EYFP-positive α-cell (bottom) from GYY mice before and after TPEN treatment. (B) Timecourses of the normalized fluorescence intensities of ZRL1 from primary α- and β-cells during 1 mM TPEN treatment (mean±s.e.m.; *n*=7 for each cell type). (C) Mean±s.e.m. fluorescence intensities of ZRL1-labeled primary α-cells and β-cells (*n*=13 for α-cells, *n*=17 for β-cells). a.u., arbitrary units. (D) Timecourse of normalized mean±s.e.m. fluorescence intensity of ZRL1 in primary α-cells during 50 mM NH_4Cl treatment (*n*=9). (E) Double immunofluorescent staining of dissociated mouse pancreatic islet cells with anti-insulin and anti-glucagon antibodies after ZRL1 labeling and TPEN quenching. The fluorescence was normalized to the basal level. ES, extracellular solution. Scale bars: 2 µm (A); 20 µm (E). ***P<0.001; n.s., not significant (Student's *t*-test).

of the TPEN-quenchable cells were δ-cells (12 out of 227 cells; Fig. S1C), and 100% of the TPEN-resistant cells were α-cells (55 cells out of 55 cells; Fig. 2E), which proves the overall specificity of TPEN quenching. Therefore, the TPEN-quenchable and TPEN-resistant cells were mostly pancreatic β-cells and α-cells, respectively.

Measuring the mass ratio of α- versus β-cells within live islets with the FQA

Because it is difficult to label the islet core with acetoxymethyl (AM) ester form of fluorescence dyes such as fluo-3 AM (Nadal et al., 1999), we tested whether ZRL1 could label all of the α- and β-cells in intact islets and whether TPEN could reach every cell inside the islet core. The results showed that both the surface and the internal islet cells were labeled with fluorescent ZRL1 (Fig. 3A; Fig. S2A), and α- and β-cells within the islets exhibited similar average fluorescence intensities before TPEN application (Fig. 3C). Compared to single-cell experiments, the quenching of β-cell ZRL1 fluorescence within the islets by TPEN was slower but could be completed within ~600 s (Fig. 3A,B). Under a spinning disc confocal microscope, we randomly selected fluorescence intensities from 20 α-cells or β-cells at the bottom and the internal planes of islets before (a_1/b_1, a_2/b_2, a_3/b_3, …, a_{20}/b_{20}) and after TPEN quenching (a_{1TPEN}/b_{1TPEN}, a_{2TPEN}/b_{2TPEN}, a_{3TPEN}/b_{3TPEN}, …, a_{20TPEN}/b_{20TPEN}) (Fig. S2). The average quenching coefficients m (α-cells) and n (β-cells) were calculated according to the formula below:

$$m = \frac{a_{1TPEN} + a_{2TPEN} + a_{3TPEN} + \ldots + a_{20TPEN}}{a_1 + a_2 + a_3 + \ldots + a_{20}} = 0.77 \pm 0.03$$

$$n = \frac{b_{1TPEN} + b_{2TPEN} + b_{3TPEN} + \ldots + b_{20TPEN}}{b_1 + b_2 + b_3 + \ldots + b_{20}} = 0.16 \pm 0.01$$

Although the absolute ZRL1 fluorescence intensity varied from cell to cell in different planes (Fig. S2B), the average quenching

Journal of Cell Science

Journal of Cell Science (2016) 129, 2462-2471 doi:10.1242/jcs.184523

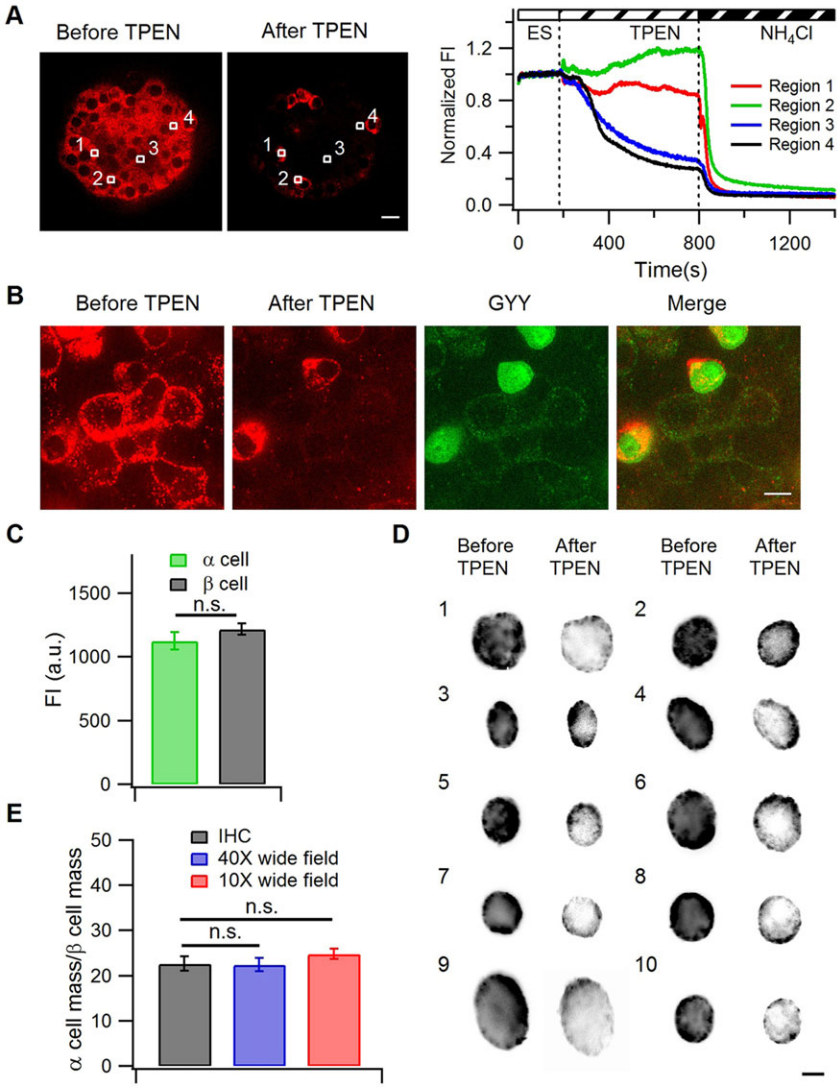

Fig. 3. ZRL1 FQA reliably reports the ratio of the α-cell to β-cell mass. (A) Left, a representative example of an intact mouse islet loaded with ZRL1 before and after TPEN quenching viewed under a confocal microscope with a 40× objective. Right, timecourses of the fluorescence in four different regions in the left images during TPEN and the following NH_4Cl perfusion. The fluorescence was normalized to the basal levels and the sampling rate was 2 Hz. ES, extracellular solution. (B) High-resolution confocal image (100× objective) of a GYY mouse pancreatic islet after ZRL1 labeling and TPEN quenching. (C) Mean±s.e.m. fluorescence intensities of ZRL1-labeled α-cells and β-cells in intact islets under a spinning disc confocal microscope with 40× objective (n=20 for α-cells, n=20 for β-cells). a.u., arbitrary units. (D) Ten representative examples of ZRL1-labeled islets before and after TPEN treatment in a 96-well plate under a wide-field microscopy with 10× objective. (E) The mean±s.e.m. mass ratios of α- and β-cells calculated by ZRL1 FQA under a wide-field microscope with a 40× objective (30 islets from six mice), or with a 10× objective (32 islets from four mice) matched those measured by immunohistochemistry (from five mice). Scale bars: 20 µm (A), 10 µm (B) or 100 µm (D). n.s., not significant (Student's t-test).

coefficients of α- and β-cells in islets were indistinguishable from that obtained from dissociated single cells (79±2% and 16±1%, respectively; mean±s.e.m.), proving the quenching of islets as a uniform process. In the following experiments, under wide-field microscopy with 40× or 10× magnification objective, we used the same quenching coefficients.

Knowing the quenching coefficients for TPEN on ZRL1 fluorescence of α- and β-cells, we calculated the ratio of the α-cell to β-cell mass within islets by simply measuring the whole islet fluorescence changes before and after TPEN quenching (FQA), as detailed in the Materials and Methods section. We conducted experiments firstly under a wide-field microscope equipped with a 40× air objective. By FQA, the ratio of the α-cell to β-cell mass in wild-type mice at 6 weeks old was 0.22±0.01 (n=30), similar to that obtained by IHC (0.23±0.02, n=150) conducted in pancreatic sections from mice of the same age (Fig. 3D). This result confirms the validity of the proposed FQA method. To further accelerate the experimental throughput, we conducted FQA experiments on individual islets that were cultured in a 96-well plate and imaged with a 10× air objective, which also gave a similar estimation of the ratio of the α-cell to β-cell mass (0.25±0.01, n=32) (Fig. 3D,E). Taken together, the FQA method yields an accurate estimation of the ratio of the α-cell to β-cell mass and can therefore be accelerated to perform automatic cellular imaging and analysis.

Application of ZRL1-TPEN in studying individual α- and β-cell function in intact islets

Next, we tested whether ZRL1 loading compromised cell function. We loaded live islet cells isolated from GYY mice with both ZRL1 and fluo-4 (a Ca^{2+} indicator), and found that glucose-stimulated Ca^{2+} transients were similar in ZRL1-loaded β-cells and ZRL1-non-loaded control cells (Fig. 4A). As compared to the ZRL1-non-loaded control cells, train depolarization also evoked exocytosis with similar kinetics in ZRL1-loaded β- or α-cells (Fig. 4B,C). This indicates that the live cells have a high tolerance to the ZRL1-loading procedure, which might be used to dissect different types of cells for functional study in intact islets.

After conducting time-lapse imaging of ZRL1- and fluo-4-stained islets incubated in 1 mM glucose-containing extracellular solution, we used TPEN to eliminate ZRL1 fluorescence in β-cells at the end of the experiment to identify α- and β-cells, respectively (Fig. 5A). Pronounced and frequent Ca^{2+} oscillations were found in most of the α-cells within the islet (90±3%, n=3; mean±s.e.m.), in contrast to small and sparse responses (28±9%, n=3) or no responses (72±9%, n=3) in β-cells (Fig. 5B).

Journal of Cell Science

Journal of Cell Science (2016) 129, 2462-2471 doi:10.1242/jcs.184523

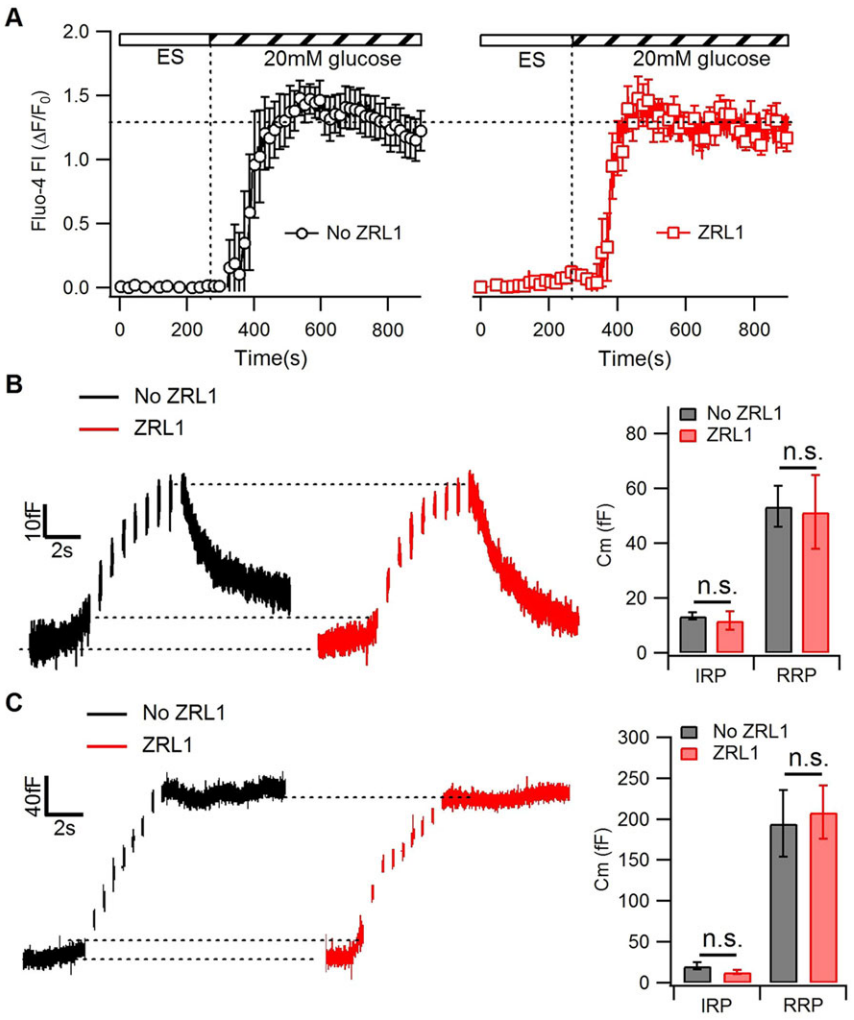

Fig. 4. Loading of ZRL1 in primary β-cells and α-cells does not affect the cell function. (A) Timecourses of mean±s.e.m. glucose-stimulated Ca^{2+} transients in control β-cells and β-cells loaded with ZRL1. Intracellular Ca^{2+} concentration was measured by loading cells with the Ca^{2+} indicator, fluo-4, and quantifying its fluorescence intensity (n=7 per group). ES, extracellular solution. (B) The average increases and decreases in the membrane capacitance (C_m) in ZRL1-treated (n=11) or non-treated (n=9) primary β-cells evoked by a train of depolarization pulses delivered by whole-cell patch-clamping. The mean±s.e.m. sizes of the immediately releasable pool (IRP) and readily releasable pool (RRP) of insulin granules in ZRL1-treated or non-treated primary β-cells are shown. (C) The average increases in the membrane capacitance (C_m) in ZRL1-treated (n=9) or non-treated (n=6) primary α-cells evoked by a train of depolarization pulses delivered by whole-cell patch-clamping. The mean±s.e.m. sizes of the IRP and RRP of glucagon granules in ZRL1-treated or non-treated primary α-cells are shown. n.s., not significant (Student's t-test).

Therefore, our method enables dissection and functional evaluation at the single α- or β-cell level.

Increases in the ratio of the α-cell to β-cell mass and function correlates with the type 2 diabetes progression

Finally, we combined ZRL1 FQA with radioimmunoassay to study changes in both the mass and functional ratios of α- and β-cells during the pathogenesis of type 2 diabetes in *db/db* mice. We selected 6- and 10-week-old *db/db* mice and compared them to age-matched C57BL/6J wild-type mice. Compared to the controls, 6-week-old *db/db* mice exhibited higher glucose levels at only 30 min after glucose injection during an intraperitoneal glucose tolerance test (IPGTT, Fig. S3A). However, the area under the curve of the glucose (AUCg) was not significantly different from the control (Fig. S3C), which indicates that these mice were at a pre-diabetic stage. At 10 weeks old, *db/db* mice had significantly elevated glycemia compared to the control mice under a fasting condition and after intraperitoneal glucose administration, and the AUCg of IPGTT of *db/db* mice was remarkably increased (Fig. S3B,C). This finding suggests that 10-week-old *db/db* mice are already in the diabetic stage, which is consistent with previous studies (Do et al., 2014; Liang et al., 2014).

At the pre-diabetic stage of *db/db* mice (6 weeks old), despite an increase in both α- and β-cell masses compared to the age-matched control mice (Fig. S3D,E), the ratio of the α-cell to β-cell mass remained unchanged as measured by IHC or FQA (Fig. 6A,C,F). We also measured glucagon release after administration of 1 mM glucose and glucose-stimulated insulin secretion (GSIS) after administration of 20 mM glucose by performing a radioimmunoassay (RIA) in islets before they were assayed with FQA. Although enhanced glucagon secretion and GSIS were also observed in islets from 6-week-old *db/db* mice (Fig. S3F,G), the glucagon-to-insulin secretion ratio was not different from the age-matched controls (Fig. 6E). Thus, the mass ratio divided by function ratio from 6-week-old *db/db* mice was similar to that of control mice (Fig. 6G). Therefore, balanced α- and β-cell functional mass is associated with overall normal glucose tolerance at this stage.

At the diabetic stage of *db/db* mice (10 weeks old), although the α- and β-cell masses were still higher than those in control mice, the relative increase in the β-cell mass (~2.1 fold of the control) was less than that of the α-cell mass (~4.6 fold of the control) (Fig. 6B,D; Fig. S3D,E). Although α-cell mass expansion in *db/db* mice was maintained from 6 to 10 weeks old, the β-cell mass expansion was significantly reduced by ~50% (Fig. S3D,E). Correspondingly, the ratio of the α-cell to β-cell mass was ~twofold that of age-matched control mice and 6-week-old *db/db* mice (Fig. 6F). In contrast, the glucagon-to-insulin secretion ratio in 10-week-old *db/db* islets was only ~150% of that of control islets (Fig. 6E). This finding led to an elevated mass divided by function ratio (Fig. 6G), which suggests an adaptive upregulation of β-cell function relative to α-cell function. When these results are taken together, in the absence of defects in functional β-cell mass, maintained expansion of α-cell mass could

Journal of Cell Science

Journal of Cell Science (2016) 129, 2462-2471 doi:10.1242/jcs.184523

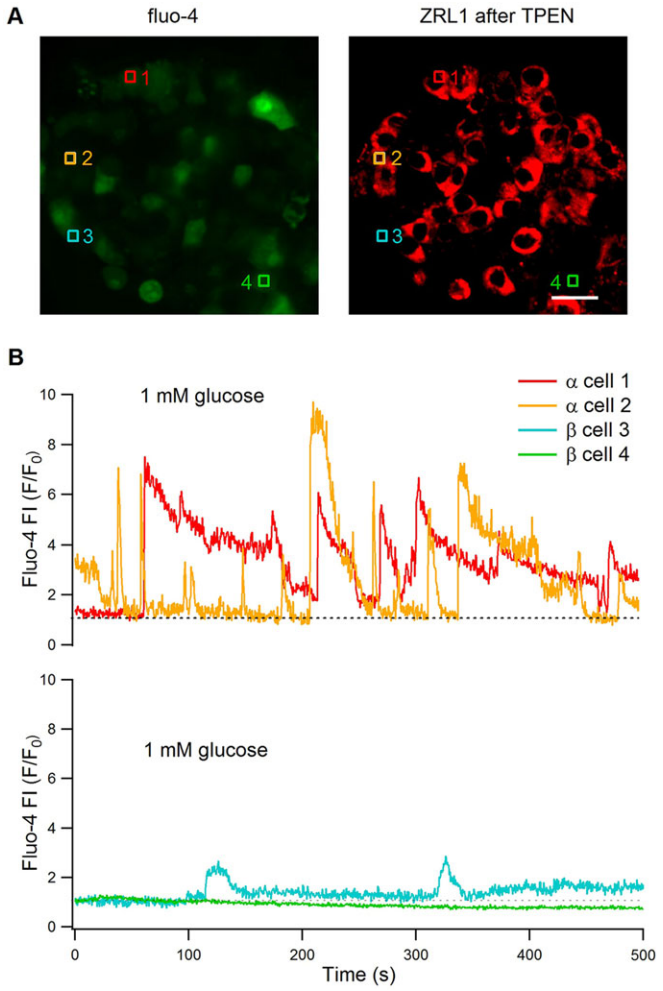

Fig. 5. The ZRL1-TPEN protocol enables identification and functional evaluation of individual α- and β-cells within the islet. (A) Left, a representative frame of time-lapse imaging of the fluo-4 fluorescence in an islet loaded with fluo-4 AM and ZRL1 and incubated with 1 mM glucose. Right, the ZRL1 fluorescence imaging of the same islet after TPEN quenching. Scale bar: 20 µm. (B) Timecourses of the normalized fluorescence intensities of fluo-4 in the four cells labeled in A. The α-cell 1 and 2 identified by ZRL1-TPEN labeling exhibited pronounced Ca^{2+} oscillation at 1 mM glucose. The β-cell 3 exhibited a small and sparse Ca^{2+} wave, whereas the β-cell 4 was completely silent all the time. The fluorescence signal was acquired with a 500-ms time interval. After 500 s imaging, TPEN was added to the islets to identify α-cells.

act as the primary factor that contributes to the disrupted glucose tolerance in *db/db* mice.

DISCUSSION

ZRL1 loading leads to accumulation of the dye in acidic, granule structures in both α- and β-cells. However, it seems paradoxical that these types of cells exhibit different sensitivities to TPEN application in α- and β-cells. Upon binding with Zn^{2+} as occurs in β-cells, ZRL1 transforms from a lactam to a ring-open form, which absorbs light centered at 569 nm and then emits red fluorescence peaked at 595 nm (Du and Lippard, 2010). ZRL1 fluorescence is turned on in solution more acidic than pH 5.4 (Du and Lippard, 2010), but the structure of fluorescent ZRL1-H^+ is unknown. Fluorescent ZRL1-H^+ might adopt a different structure as compared to fluorescent ZRL1 bound with both Zn^{2+} and H^+, which might explain the different responses of ZRL1-labeled α- and β-cells in the TPEN-quenching experiment.

The ZRL1-TPEN-based FQA method developed here can be used to dissect and evaluate function of single α- or β-cells in intact islets. As ZRL1 is a red fluorophore, it can be easily combined with popular green Ca^{2+} fluorophores such as fluo-4. As shown in Fig. 5, it enables real-time measurements of Ca^{2+} dynamics of individual α- or β-cells within an islet without the need of transgenic mice in which specific islet cell types are fluorescently labeled. Thus, it might facilitate parallel comparisons of glucose-evoked responses in α- and β-cells within islets during diabetes progression in different animal models. ZRL1 can also be combined with transgenic mice in which pancreatic δ-cells are labeled with EGFP. Under such a circumstance, in addition to the visualization of the three-dimensional assembly of α-, β- and δ-cells within the islets, the functions of all islet cells in the physiological-relevant environments can also be evaluated with far-red Ca^{2+} fluorophores (Oheim et al., 2014).

Unlike a conventional IHC method, the FQA method cannot be used to estimate the size of islets *in vivo*, neither can it differentiate size differences between different islets. However, it is fast and can be easily adapted to automatic imaging systems (Fig. 3E). Thus, it could serve as a fast method to pre-screen for possible changes in the ratio of the α-cell to β-cell mass in islets. Pancreatic δ-cells are also labeled by ZRL1 in a TPEN-quenchable manner (Fig. S1C), despite the underlying mechanism remaining unclear. This might lead to overestimation of β-cell contribution to the total ZRL1 fluorescence in live islets. However, δ-cells comprise less than 10% of total pancreatic islet content (Leiter et al., 1979). In agreement with a minor contribution of δ-cells, the ratio of the α-cell to β-cell mass in live islets calculated based on FQA is not significantly different from that obtained by IHC from pancreas slices isolated from mice with the same age in multiple experimental trials (Figs 3D and 6F). Thus, we conclude that FQA can generate approximate estimations of the ratio of the α-cell to β-cell mass to those measured by IHC in pancreatic slices from mice of similar conditions. As live islet functions can be measured before the FQA, our method enables fast measurement of α-cell to β-cell mass and function ratios in the same live islets.

Glucose or arginine stimulates hypersecretion of both glucagon and insulin in islets that are isolated from 2- to 3-month-old *db/db* mice (Laube et al., 1973). Here, we showed that glucagon and insulin hypersecretion appeared even earlier in 6-week-old *db/db* mouse islets (Fig. S3F,G), which is possibly due to uniform increases in the α- and β-cell area because of islet expansion (Fig. S3D,E). At a later (10-week-old) stage, the maintained upregulation of the α-cell mass but reduced upregulation of the β-cell mass resulted in an increase in the ratio of the α-cell to β-cell mass compared to that in the 6-week-old *db/db* mice. This finding resembles those from a study conducted in non-human primates in which obesity promoted a small increase in β-cell mass and a concomitant large increase in α-cell mass (Guardado-Mendoza et al., 2013). Selective α-cell expansion and β-cell loss is also found in type 2 diabetes patients (Yoon et al., 2003), which suggests that the mechanism found here could be conserved among different species. However, whether changes in the islet cell mass lead to corresponding changes in function was not determined in either case (Guardado-Mendoza et al., 2013; Yoon et al., 2003). In ten-week-old *db/db* mice, the increase in the α-cell to β-cell function ratio was less than that of the ratio of the α-cell to β-cell mass, which reflects that individual β-cell function was enhanced rather than compromised relative to individual α-cell function. This finding fits with the previous report of insulin hypersecretion from isolated β-cells in 8-week-old *db/db* mice (Liang et al., 2014). Decreased

Journal of Cell Science (2016) 129, 2462-2471 doi:10.1242/jcs.184523

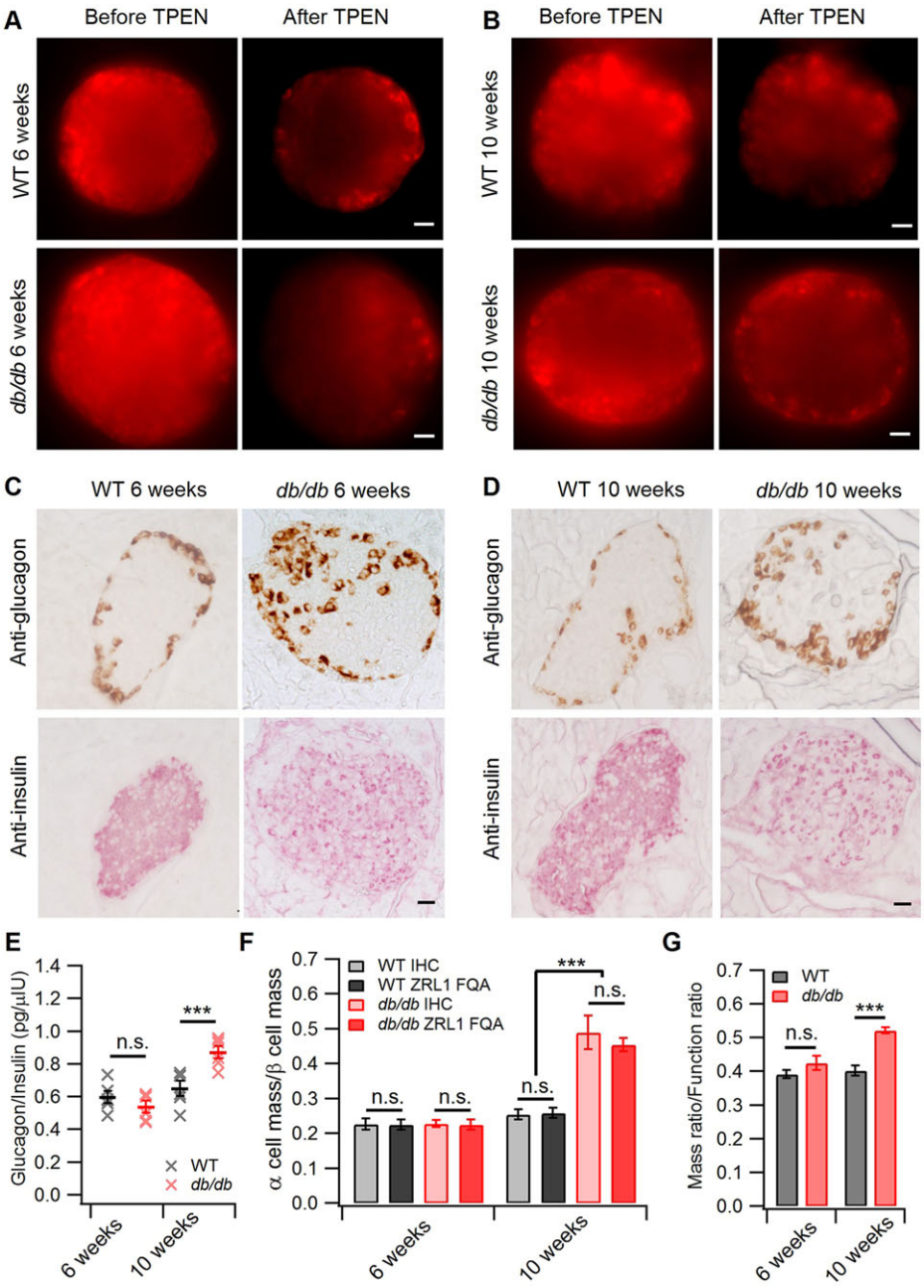

Fig. 6. ZRL1 FQA combined with a functional test to evaluate the changes in the mass and functional ratios of the α-cells to β-cells in *db/db* mice. (A,B) Representative ZRL1 images of islets from 6-week-old (A) or 10-week-old (B) wild-type (WT) and *db*/*db* mice before and after TPEN quenching, respectively. (C,D) Immunohistochemistry images of a pair of serial pancreatic sections of 6-week-old (C) or 10-week-old (D) wild-type and *db*/*db* mice with anti-glucagon and anti-insulin antibodies, respectively. (E) Mean±s.e.m. functional ratio of α- and β-cells (secreted glucagon versus GSIS) in 6- and 10-week-old wild-type and *db*/*db* mice (n=6 per group). (F) The ratio of the α-cell to β-cell mass in 6- and 10-week-old wild-type and *db*/*db* mice calculated by ZRL1 FQA (30 islets from 6 mice per group) or by immunohistochemistry (n=5 per group). (G) The normalized mass ratio versus functional ratio in 6- and 10-week-old wild-type and *db*/*db* mice. Scale bars: 10 μm. Data are ***P<0.001; n.s., not significant (Student's t-test).

GSIS from *db/db* mice is observed only at an even later stage (at 13 to 18 weeks old) (Do et al., 2014), which further leads to hyperglycemia, partially due to the suppression effect of insulin on glucagon secretion being impaired (Unger and Orci, 2010). Overall, our data placed the upregulation of α-cell mass at a stage where β-cells exhibit normal or even enhanced function, which suggests that the upregulation of α-cell mass could be a primary driving force for hyperglycemia in animal models and human type 2 diabetes patients. The underlying mechanism could be an enrichment of some cytokines and microRNAs in subjects that have obesity, insulin resistance or type 2 diabetes (Daniele et al., 2014; Guardado-Mendoza et al., 2013; Poy et al., 2009), which selectively preserve the upregulation of α-cell mass (Ellingsgaard et al., 2008; Poy et al., 2009).

Consistent with this idea, most patients with glucagon-secreting pancreatic neuroendocrine tumors are diabetic (Eldor et al., 2011). Conversely, the elimination of β-cell mass in glucagon-receptor-null mice does not cause diabetes (Lee et al., 2011; Sorensen et al., 2006; Yang et al., 2011). In addition, genetic modifications that reduced glucagon release (Wang et al., 2015) or eliminated the function of glucagon (Lee et al., 2014) protected high-fat diet-fed mice against hyperglycemia and insulin resistance. The most intriguing example is the synaptotagmin-VII-knockout (KO) mice. Despite the significantly reduced GSIS from β-cells (Gustavsson et al., 2008) and glucagon-like peptide-1 released from the gut (Gustavsson et al., 2011b), compared to control mice, synaptotagmin-VII-KO mice are resistant to a high-fat diet. This phenomenon is due to a much more severe reduction in glucagon secretion from α-cells in the KO mice (Gustavsson et al., 2011a). Therefore, the balance in the functional α- and β-cell masses maintains blood glucose homeostasis *in vivo*. To pinpoint the initial and universal driving force that underlies

Journal of Cell Science

Journal of Cell Science (2016) 129, 2462-2471 doi:10.1242/jcs.184523

imbalanced hormone releases during type 2 diabetes progression, we need to investigate α- and β-cell masses and functions in diabetic animal models at multiple time points. The fast, non-biased ZRL1 FQA method presented here shall have wide application in this regard.

MATERIALS AND METHODS

Mice

The *db/db* mice were from Cavens Experimental Animal Co., Changzhou, China. The *GluCre-ROSA26EYFP* (*GYY*) mice were kindly provided by Herbert Y. Gaisano from the University of Toronto, Toronto, Canada. The mice were maintained and handled according to the institutional guidelines for the use of live animals in teaching and research at Peking University, which is accredited by the AAALAC. Male mice were used in all the experiments performed in this study.

Isolation of mouse pancreatic islets and dissociation of islets into single cells

Primary islets were isolated from mice as previously described (Liang et al., 2014). After being washed in Krebs-Ringer bicarbonate buffer (KRBB) solution (135 mM NaCl, 4.7 mM KCl, 10 mM HEPES pH 7.4, 3 mM glucose, 1.2 mM KH_2PO_4 and 5 mM $NaHCO_3$) with 0.1% BSA, the islets were digested with 0.025% trypsin (Life Technologies) for 5 min at 37°C. The cells were then plated on coverslips that were coated with poly-L-lysine and maintained in a 37°C, 5% CO_2 incubator for 24–48 h in modified RPMI 1640 medium.

Loading of ZRL1 alone or with other dyes

First, we incubated islet cells with various concentrations of ZRL1 in KRBB solution for 40 min at 37°C, which yielded 20 µM ZRL1 as the saturating loading concentration (Fig. 1B). Next, we loaded cells with 20 µM ZRL1 for different periods of time, which gave 30–40 min as the saturating loading time (Fig. 1C). Subsequently, dispersed cells were preloaded with 20 µM ZRL1 in KRBB solution for 30–40 min at 37°C before experiments. For the islet experiments, the protocol was the same except the loading time was extended to 1 h.

To double-label dispersed cells with FFN511 (Sigma) and ZRL1, the cells were preloaded with ZRL1 first and then with 7 µM FFN511 in KRBB for 10–15 min at 37°C. For the Ca^{2+} imaging experiment, fluo-4 AM (Invitrogen, USA) loading was conducted at room temperature to reduce its accumulation in organelles. Dissociated islet cells isolated from GYY mice were preloaded with 1 µM fluo-4 AM for 1 h with or without ZRL1 loading (Fig. 4A). Pancreatic islets were preloaded with 5 µM fluo-4 AM and 20 µM ZRL1 for 1 h before experiments (Fig. 5).

Fluorescence imaging setups

Labeled cells and islets were imaged either under a total internal reflection fluorescence (TIRF) microscope, a spinning disc confocal microscope or a wide-field microscope. An Olympus IX81 inverted TIRF microscope equipped with a 150×, 1.45 numerical aperture (NA) oil-immersion objective was used in Figs 1B,D and 2A–D. The spinning disc confocal microscope was equipped with a 40×, 0.95 NA air objective (Olympus) for data shown in Figs 1C, 2E, 3A, 5A, Fig. S1A,C, S2A, and a 100×, 1.35 NA oil-immersion objective (Olympus) for data shown in Fig. 3B, Fig. S1B. We used a wide-field microscope (Olympus) equipped with a 40×, 0.95 NA air objective for Figs 4A and 6A,B; and a wide-field microscope equipped with a 10×, 0.4 NA air objective for Fig. 3D,E.

We used a 473-nm laser to excite fluo-4, FFN511, EYFP and collected the emission photons with a single-band bandpass filter at 525/40 nm, and we used a 561-nm laser to excite ZRL1 fluorescence and collected the emissions with a single-band bandpass filter at 607/36 nm. Emission photons were collected with an Andor iXon3 888 electron-multiplying charge-coupled device (EMCCD) camera in the TIRF and the wide-field microscope, or with an Andor iXon3 897 EMCCD camera in the confocal microscope. All systems were controlled by MetaMorph (Molecular Devices).

Quantification of ZRL1 fluorescence puncta in α-cells

After ZRL1 labeling, *z*-stack imaging of EYFP-positive α-cells from GYY mice were taken under the spinning disc confocal microscope, with a 0.2-µm step length. The ZRL1 fluorescence puncta in all the stacks were quantified automatically with the software described previously (Yuan et al., 2015).

Immunofluorescence

Dissociated islet cells were fixed in 4% paraformaldehyde for 20 min and permeabilized in 0.1 M PBS with 0.3% (v/v) Triton X-100 for 30 min at room temperature. After incubation in 5% BSA and 0.15% Triton X-100 blocking solution for 1 h, the cells were treated with primary antibodies for 1 h at 4°C, washed with PBS and further incubated with the appropriate fluorochrome-conjugated secondary antibodies for 1 h. Primary antibodies included a guinea pig anti-insulin antibody (1:200, catalog no. ab7842, Abcam, UK), a mouse anti-glucagon antibody (1:200, catalog no. ab10988, Abcam, UK) and a mouse anti-somatostatin antibody (1:200, catalog no. ab140665, Abcam, UK). After being thoroughly washed with PBS, immunofluorescence images of the cells were acquired with the confocal microscope described above.

ZRL1 FQA

ZRL1-loaded islets or dissociated islet cells were treated with TPEN (Tokyo Chemical Industry Co., Ltd., Japan) to quench the ZRL1 fluorescence in the β-cells. Because we always did the TPEN quenching at the end of a functional experiment, we selected a 1 mM concentration to ensure fastest quenching of ZRL1 in cells and islets (Fig. 1D). Before and after adding the TPEN, fluorescent images were captured under either a confocal microscope or a wide-field fluorescence microscope. Images were taken with a 40×, NA 0.95 AIR objective on the wide-field fluorescent microscope under the same experimental conditions (exposure time, EM gain and laser intensity) that were used for estimating the mass ratio of α-cells to β-cells (R) in a single islet according to the following equation:

$$R = \frac{x}{y} = \frac{x'}{y'}, \tag{1}$$

where x and y represent the α- and β-cell masses within an islet, respectively, and x' and y' represent the total ZRL1 fluorescence intensities from α- and β-cells within the same islet, respectively. This equation holds as long as the mean total ZRL1 fluorescence intensity from a single β-cell is approximately the same as that from a single α-cell (Figs 2C and 3C), and the quenching coefficients of α- and β-cells remains stable at different focal planes (Fig. S2). Therefore, we could calculate x' and y' as follows:

$$x' + y' = F, \tag{2}$$

$$mx' + ny' = F_{\mathrm{TPEN}}, \tag{3}$$

where F and F_{TPEN} denote the whole islet ZRL1 fluorescence before TPEN quenching and after TPEN quenching, respectively, and m and n represent the quenching coefficients measured from individual α- and β-cells, respectively.

By combining Eqns 1, 2 and 3, we could derive

$$R = \frac{nF - F_{\mathrm{TPEN}}}{F_{\mathrm{TPEN}} - mF}. \tag{4}$$

F and F_{TPEN} could be directly measured from the islet, and the average m and n were obtained from multiple fluorescence intensity measurements from single α- or β-cells before and after TPEN quenching. For high-content imaging, each well in a 96-well plate was filled with a single islet and imaged sequentially with a 10×, NA 0.40 AIR objective under wide-field illumination.

Measurement of the ratio of the α-cell to β-cell mass by IHC

Pancreases from wild-type and *db/db* mice were dissected, fixed in 4% paraformaldehyde solution and embedded in paraffin. Serial sections of 5 µm were obtained from different levels of the blocks. For each pair of serial sections, one deparaffinized section was incubated with a mouse anti-insulin antibody (1:200, catalog no. ZM-0155, ZSGB-BIO, Beijing, China),

and the other was stained with a rabbit anti-glucagon antibody (1:200, catalog no. ZA-0119, ZSGB-BIO, Beijing, China). The sections were then incubated with an alkaline-phosphatase-conjugated goat anti-mouse-IgG or horseradish-peroxidase-conjugated goat anti-rabbit-IgG antibodies and developed with naphthol AS-BI phosphate (AP-Red, ZSGB-BIO, Beijing, China) or 3,3-diaminobenzidine (DAB, ZSGB-BIO, Beijing, China), respectively, which stained insulin-positive cells a red–brown color or glucagon-positive cells a golden brown color. The images of the pair of serial sections were merged to evaluate the ratio of the glucagon-positive area to the insulin-positive area with the ImagePro Plus 6.0 software, for the ratio of the α-cell to β-cell mass. For each group, at least 150 islets from five mice were analyzed.

Electrophysiology

Secretion from individual β-cells was measured by whole-cell voltage clamp in the absence or presence of ZRL1 loading. Secretion from individual α-cells was measured by whole-cell voltage clamp in the absence or presence of ZRL1 loading with 10 µM forskolin (Sigma) in KRBB solution. Changes in the membrane capacitance were recorded after a train of depolarization pulses from −70 to 0 mV. The stimulus train (Cm5+8) consisted of five 50-ms and eight 500-ms depolarization pulses to stimulate release from the immediately releasable pool (IRP) and readily releasable pool (RRP). The interpulse interval was 100 ms. The intracellular solution contained 152 mM $CsCH_3SO_3$, 10 mM CsCl, 10 mM KCl, 1 mM $MgCl_2$ and 5 mM HEPES, with pH adjusted to 7.35 using CsOH.

Intraperitoneal glucose tolerance test

After fasting overnight with free access to water in clean cages, the mice were injected with 1.5 mg/g body weight of D-glucose intraperitoneally. Blood glucose was measured from the tail tip using an ACCU-CHEK® Active blood glucose meter (Roche Diagnostics) at 0, 15, 30, 60 and 120 min post injection.

Insulin and glucagon secretion test by radioimmunoassay

Thirty islets from each wild-type and *db/db* mouse were pre-incubated in 500 µl of KRBB solution for 30 min at 37°C and then transferred into another 500 µl of KRBB solution supplemented with 20 mM glucose for 30 min. At the end of the incubation, 100 µl of incubation medium was withdrawn for insulin measurement. Next, the islets were transferred to a new 500 µl of KRBB solution supplemented with 1 mM glucose for 30 min. At the end of the incubation period, 200 µl of incubation medium was withdrawn for glucagon measurement. Secreted insulin and glucagon was quantified by RIA with a human insulin and glucagon radioimmunoassay kit (Beijing North Institution of Biological Technology, China) according to the manufacturer's specifications. Then, the islets were used to measure the mass ratio of the α- and β-cells with ZRL1 FQA.

Statistical analysis

All of the data were analyzed using IgorPro software (Wavemetrics, Lake Oswego, OR). The average results are presented as the mean±s.e.m. from the number of experiments indicated. Statistical significance was evaluated using Student's *t*-test for single Gaussian distributed datasets or the Mann–Whitney rank sum test for non-single Gaussian distributed datasets. The asterisks *, ** and *** denote statistical significance with *P* values of less than 0.05, 0.01, and 0.001, respectively. All of the data were from at least three independent experiments.

Acknowledgements

We thank Stephen J. Lippard and Robert J. Radford for providing the ZRL1 reagent and for their comments on the manuscript.

Competing interests

The authors declare no competing or financial interests.

Author contributions

Y.W., Y.L. and L.C. designed research; Y.W., C.H. and W.Z. performed research; Y.W., Y.L. and L.C. analyzed data; and Y.W., Z.W., Y.L. and L.C. wrote the paper.

Funding

This work was supported by grants from the National Natural Science Foundation of China [grant numbers 81222020, 31221002, 31327901, 31570839, 31301186, 31471034]; the Beijing Municipal Science and Technology Commission [grant numbers 7121008, 7152079]; the Major State Basic Research Program of China [grant numbers 2013CB531200, 2011CB910203]; and the National Key Technology Research and Development Program [grant number SQ2011SF11B01041].

Supplementary information

Supplementary information available online at
http://jcs.biologists.org/lookup/suppl/doi:10.1242/jcs.184523/-/DC1

References

Campbell, J. E. and Drucker, D. J. (2013). Pharmacology, physiology, and mechanisms of incretin hormone action. *Cell Metab.* **17**, 819-837.

Cobelli, C., Toffolo, G. M., Dalla Man, C., Campioni, M., Denti, P., Caumo, A., Butler, P. and Rizza, R. (2007). Assessment of beta-cell function in humans, simultaneously with insulin sensitivity and hepatic extraction, from intravenous and oral glucose tests. *Am. J. Physiol. Endocrinol. Metab.* **293**, E1-E15.

Colvin, R. A., Bush, A. I., Volitakis, I., Fontaine, C. P., Thomas, D., Kikuchi, K. and Holmes, W. R. (2008). Insights into Zn2+ homeostasis in neurons from experimental and modeling studies. *Am. J. Physiol. Cell Physiol.* **294**, C726-C742.

D'Alessio, D. (2011). The role of dysregulated glucagon secretion in type 2 diabetes. *Diabetes Obes. Metab.* **13** Suppl 1, 126-132.

Daniele, G., Guardado Mendoza, R., Winnier, D., Fiorentino, T. V., Pengou, Z., Cornell, J., Andreozzi, F., Jenkinson, C., Cersosimo, E., Federici, M. et al. (2014). The inflammatory status score including IL-6, TNF-alpha, osteopontin, fractalkine, MCP-1 and adiponectin underlies whole-body insulin resistance and hyperglycemia in type 2 diabetes mellitus. *Acta Diabetol.* **51**, 123-131.

Do, O. H., Low, J. T., Gaisano, H. Y. and Thorn, P. (2014). The secretory deficit in islets from db/db mice is mainly due to a loss of responding beta cells. *Diabetologia* **57**, 1400-1409.

Du, P. and Lippard, S. J. (2010). A highly selective turn-on colorimetric, red fluorescent sensor for detecting mobile zinc in living cells. *Inorg. Chem.* **49**, 10753-10755.

Eldor, R., Glaser, B., Fraenkel, M., Doviner, V., Salmon, A. and Gross, D. J. (2011). Glucagonoma and the glucagonoma syndrome - cumulative experience with an elusive endocrine tumour. *Clin. Endocrinol.* **74**, 593-598.

Ellingsgaard, H., Ehses, J. A., Hammar, E. B., Van Lommel, L., Quintens, R., Martens, G., Kerr-Conte, J., Pattou, F., Berney, T., Pipeleers, D. et al. (2008). Interleukin-6 regulates pancreatic alpha-cell mass expansion. *Proc. Natl. Acad. Sci. USA* **105**, 13163-13168.

Guardado-Mendoza, R., Jimenez-Ceja, L., Majluf-Cruz, A., Kamath, S., Fiorentino, T. V., Casiraghi, F., Velazquez, A. O. C., DeFronzo, R. A., Dick, E., Davalli, A. et al. (2013). Impact of obesity severity and duration on pancreatic beta- and alpha-cell dynamics in normoglycemic non-human primates. *Int. J. Obes.* **37**, 1071-1078.

Gustavsson, N., Lao, Y., Maximov, A., Chuang, J.-C., Kostromina, E., Repa, J. J., Li, C., Radda, G. K., Sudhof, T. C. and Han, W. (2008). Impaired insulin secretion and glucose intolerance in synaptotagmin-7 null mutant mice. *Proc. Natl. Acad. Sci. USA* **105**, 3992-3997.

Gustavsson, N., Seah, T., Lao, Y., Radda, G. K., Südhof, T. C. and Han, W. (2011a). Delayed onset of hyperglycaemia in a mouse model with impaired glucagon secretion demonstrates that dysregulated glucagon secretion promotes hyperglycaemia and type 2 diabetes. *Diabetologia* **54**, 415-422.

Gustavsson, N., Wang, Y., Kang, Y., Seah, T., Chua, S., Radda, G. K. and Han, W. (2011b). Synaptotagmin-7 as a positive regulator of glucose-induced glucagon-like peptide-1 secretion in mice. *Diabetologia* **54**, 1824-1830.

Henquin, J.-C., Accili, D., Ahrén, B., Boitard, C., Seino, S. and Cerasi, E. (2011). Long in the shade, glucagon re-occupies centre court. *Diabetes Obes. Metab.* **13** Suppl 1, v-viii.

Jamison, R. A., Stark, R., Dong, J., Yonemitsu, S., Zhang, D., Shulman, G. I. and Kibbey, R. G. (2011). Hyperglucagonemia precedes a decline in insulin secretion and causes hyperglycemia in chronically glucose-infused rats. *Am. J. Physiol. Endocrinol. Metab.* **301**, E1174-E1183.

Koh, D.-S., Cho, J.-H. and Chen, L. (2012). Paracrine interactions within islets of Langerhans. *J. Mol. Neurosci.* **48**, 429-440.

Laube, H., Fussgänger, R. D., Maier, V. and Pfeiffer, E. F. (1973). Hyperglucagonemia of the isolated perfused pancreas of diabetic mice (db-db). *Diabetologia* **9**, 400-402.

Lee, Y., Wang, M.-Y., Du, X. Q., Charron, M. J. and Unger, R. H. (2011). Glucagon receptor knockout prevents insulin-deficient type 1 diabetes in mice. *Diabetes* **60**, 391-397.

Lee, Y., Berglund, E. D., Yu, X., Wang, M.-Y., Evans, M. R., Scherer, P. E., Holland, W. L., Charron, M. J., Roth, M. G. and Unger, R. H. (2014). Hyperglycemia in rodent models of type 2 diabetes requires insulin-resistant alpha cells. *Proc. Natl. Acad. Sci. USA* **111**, 13217-13222.

Journal of Cell Science

Leiter, E. H., Gapp, D. A., Eppig, J. J. and Coleman, D. L. (1979). Ultrastructural and morphometric studies of delta cells in pancreatic islets from C57BL/Ks diabetes mice. *Diabetologia* **17**, 297-309.
Li, Y. V. (2014). Zinc and insulin in pancreatic beta-cells. *Endocrine* **45**, 178-189.
Liang, K., Du, W., Lu, J., Li, F., Yang, L., Xue, Y., Hille, B. and Chen, L. (2014). Alterations of the Ca(2)(+) signaling pathway in pancreatic beta-cells isolated from db/db mice. *Protein Cell* **5**, 783-794.
Nadal, A., Quesada, I. and Soria, B. (1999). Homologous and heterologous asynchronicity between identified alpha-, beta- and delta-cells within intact islets of Langerhans in the mouse. *J. Physiol.* **517**, 85-93.
Nolan, C. J., Madiraju, M. S. R., Delghingaro-Augusto, V., Peyot, M.-L. and Prentki, M. (2006). Fatty acid signaling in the beta-cell and insulin secretion. *Diabetes* **55** Suppl 2, S16-S23.
Oheim, M., van't Hoff, M., Feltz, A., Zamaleeva, A., Mallet, J.-M. and Collot, M. (2014). New red-fluorescent calcium indicators for optogenetics, photoactivation and multi-color imaging. *Biochim. Biophys. Acta* **1843**, 2284-2306.
Poy, M. N., Hausser, J., Trajkovski, M., Braun, M., Collins, S., Rorsman, P., Zavolan, M. and Stoffel, M. (2009). miR-375 maintains normal pancreatic alpha- and beta-cell mass. *Proc. Natl. Acad. Sci. USA* **106**, 5813-5818.
Quesada, I., Tuduri, E., Ripoll, C. and Nadal, A. (2008). Physiology of the pancreatic alpha-cell and glucagon secretion: role in glucose homeostasis and diabetes. *J. Endocrinol.* **199**, 5-19.
Quoix, N., Cheng-Xue, R., Guiot, Y., Herrera, P. L., Henquin, J.-C. and Gilon, P. (2007). The GluCre-ROSA26EYFP mouse: a new model for easy identification of living pancreatic alpha-cells. *FEBS Lett.* **581**, 4235-4240.
Sorensen, H., Winzell, M. S., Brand, C. L., Fosgerau, K., Gelling, R. W., Nishimura, E. and Ahren, B. (2006). Glucagon receptor knockout mice display increased insulin sensitivity and impaired beta-cell function. *Diabetes* **55**, 3463-3469.
Unger, R. H. and Cherrington, A. D. (2012). Glucagonocentric restructuring of diabetes: a pathophysiologic and therapeutic makeover. *J. Clin. Invest.* **122**, 4-12.
Unger, R. H. and Orci, L. (2010). Paracrinology of islets and the paracrinopathy of diabetes. *Proc. Natl. Acad. Sci. USA* **107**, 16009-16012.
Wang, L., Luk, C. T., Cai, E. P., Schroer, S. A., Allister, E. M., Shi, S. Y., Wheeler, M. B., Gaisano, H. Y. and Woo, M. (2015). PTEN deletion in pancreatic alpha-cells protects against high-fat diet–induced hyperglucagonemia and insulin resistance. *Diabetes* **64**, 147-157.
Weir, G. C. and Bonner-Weir, S. (2004). Five stages of evolving beta-cell dysfunction during progression to diabetes. *Diabetes* **53** Suppl 3, S16-S21.
Yang, J., MacDougall, M. L., McDowell, M. T., Xi, L., Wei, R., Zavadoski, W. J., Molloy, M. P., Baker, J. D., Kuhn, M., Cabrera, O. et al. (2011). Polyomic profiling reveals significant hepatic metabolic alterations in glucagon-receptor (GCGR) knockout mice: implications on anti-glucagon therapies for diabetes. *BMC Genomics* **12**, 281.
Yoon, K. H., Ko, S. H., Cho, J. H., Lee, J. M., Ahn, Y. B., Song, K. H., Yoo, S. J., Kang, M. I., Cha, B. Y., Lee, K. W. et al. (2003). Selective beta-cell loss and alpha-cell expansion in patients with type 2 diabetes mellitus in Korea. *J. Clin. Endocrinol. Metab.* **88**, 2300-2308.
Yuan, T., Lu, J., Zhang, J., Zhang, Y. and Chen, L. (2015). Spatiotemporal detection and analysis of exocytosis reveal fusion "hotspots" organized by the cytoskeleton in endocrine cells. *Biophys. J.* **108**, 251-260.

SUPPLEMENTARY MATERIAL

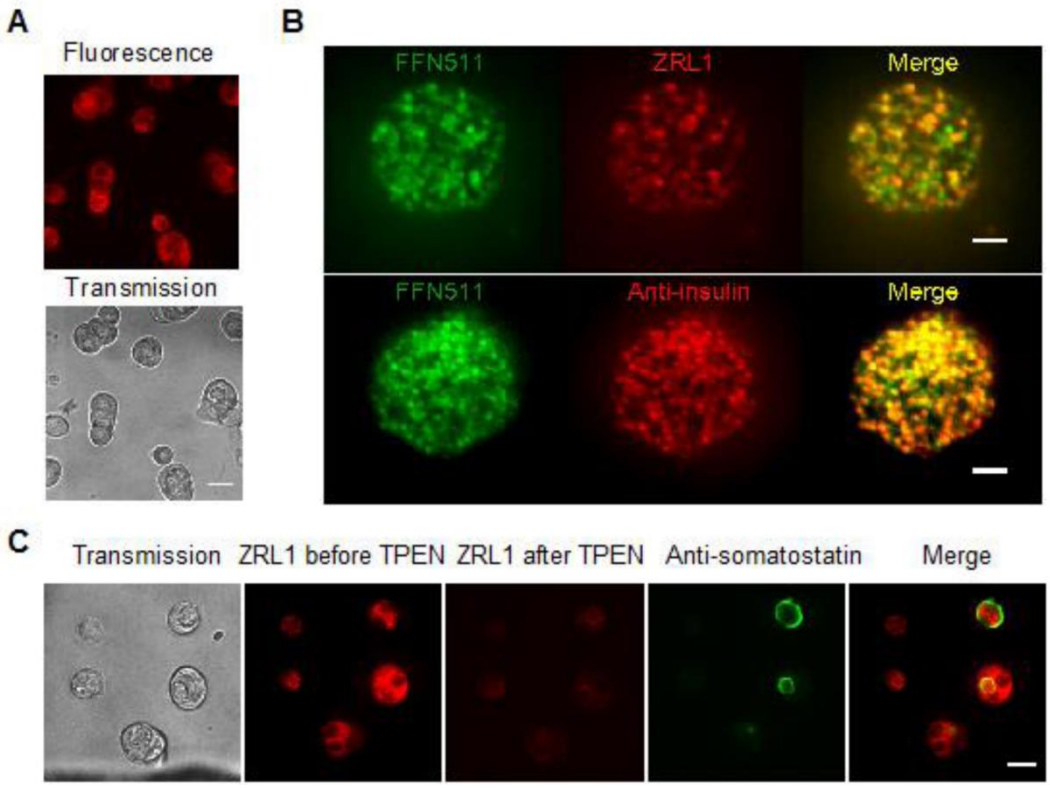

Fig. S1. ZRL1 could label all dissociated islet cells. (A) A representative image of dissociated islet cells labeled with ZRL1 under the wide-field microscope. Scale bars represent 20 μm. **(B)** ZRL1 labels insulin granules in primary β cells. Upper, confocal imaging of FFN511 (left) and ZRL1 (middle) signals in an EYFP negative living islet cell from GYY mice after sequential incubation with ZRL1 and FFN511. Lower, confocal imaging of FFN511 (left) and immunofluorescence with anti-insulin antibody (middle) in an EYFP negative fixed islet cell from GYY mice after FFN511 labeling followed with immunostaining. Scale bars represent 2 μm. **(C)** ZRL1 labels primary δ cells, which fluorescence could be quenched by TPEN. A representative example of immunofluorescent staining of dissociated mouse pancreatic islet cells with anti-somatostatin antibodies after ZRL1 labeling, with and without TPEN quenching. The scale bar represents 20 μm.

Journal of Cell Science • Supplementary information

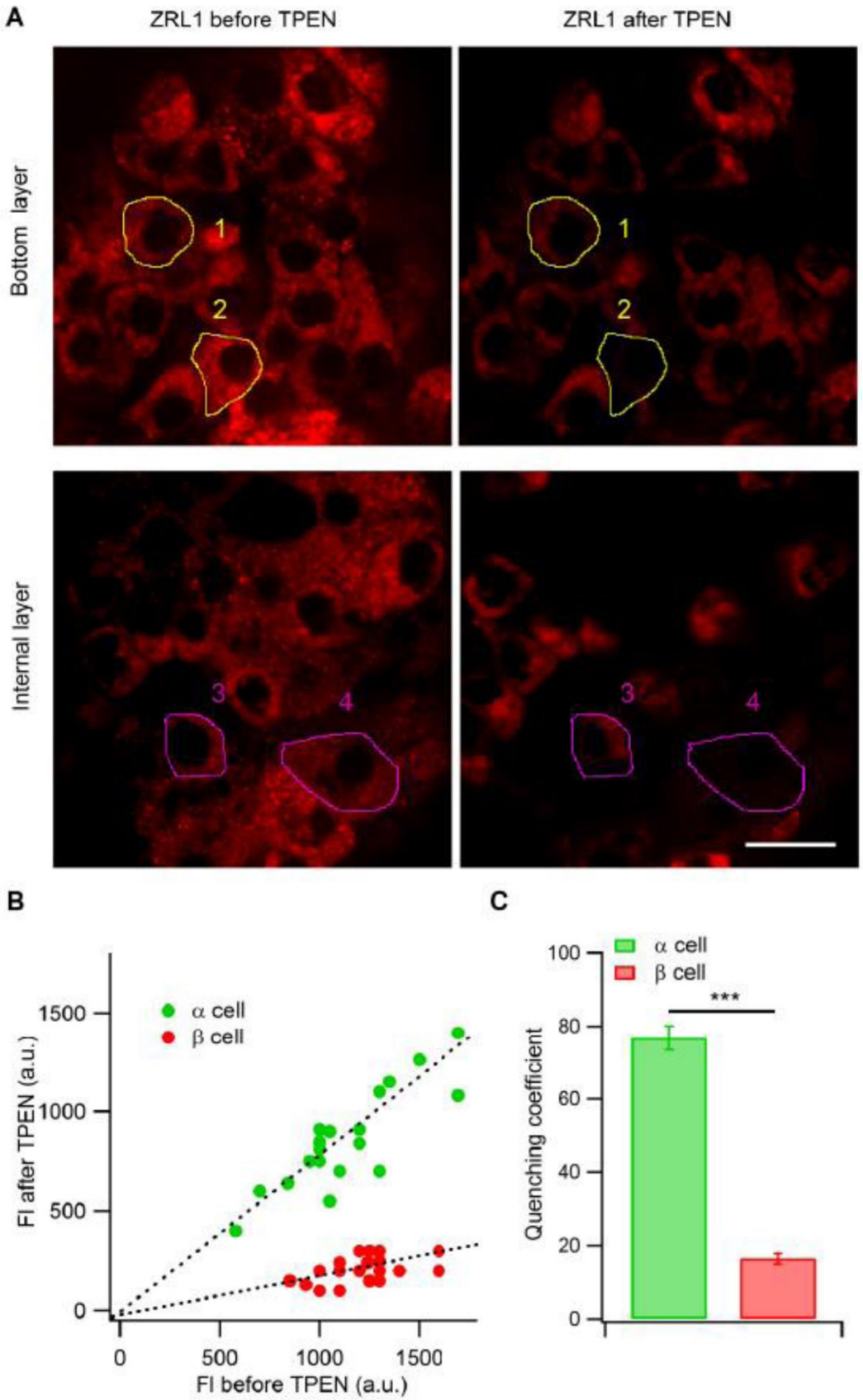

Journal of Cell Science • Supplementary information

Fig. S2. Calculation of ZRL1 quenching coefficients in α-cells and β-cells. (A) Representative bottom layer and internal layer (40 μm inside) of ZRL1 imaging of islets before and after TPEN quenching. Cell 1 and 3 are two α-cell examples, while cell 2 and 4 are two β-cell examples. ZRL1 fluorescence intensity of each cell before and after TPEN quenching was measured in the selected area. The scale bar represents 20 μm. **(B)** ZRL1 fluorescence intensity after TPEN quenching positively linearly correlated with that before TPEN quenching in α-cells or in β-cells. Each spot represents data from one cell. $n = 20$ for each cell type. **(C)** The average quenching coefficient calculated based on **(B).**

Journal of Cell Science • Supplementary information

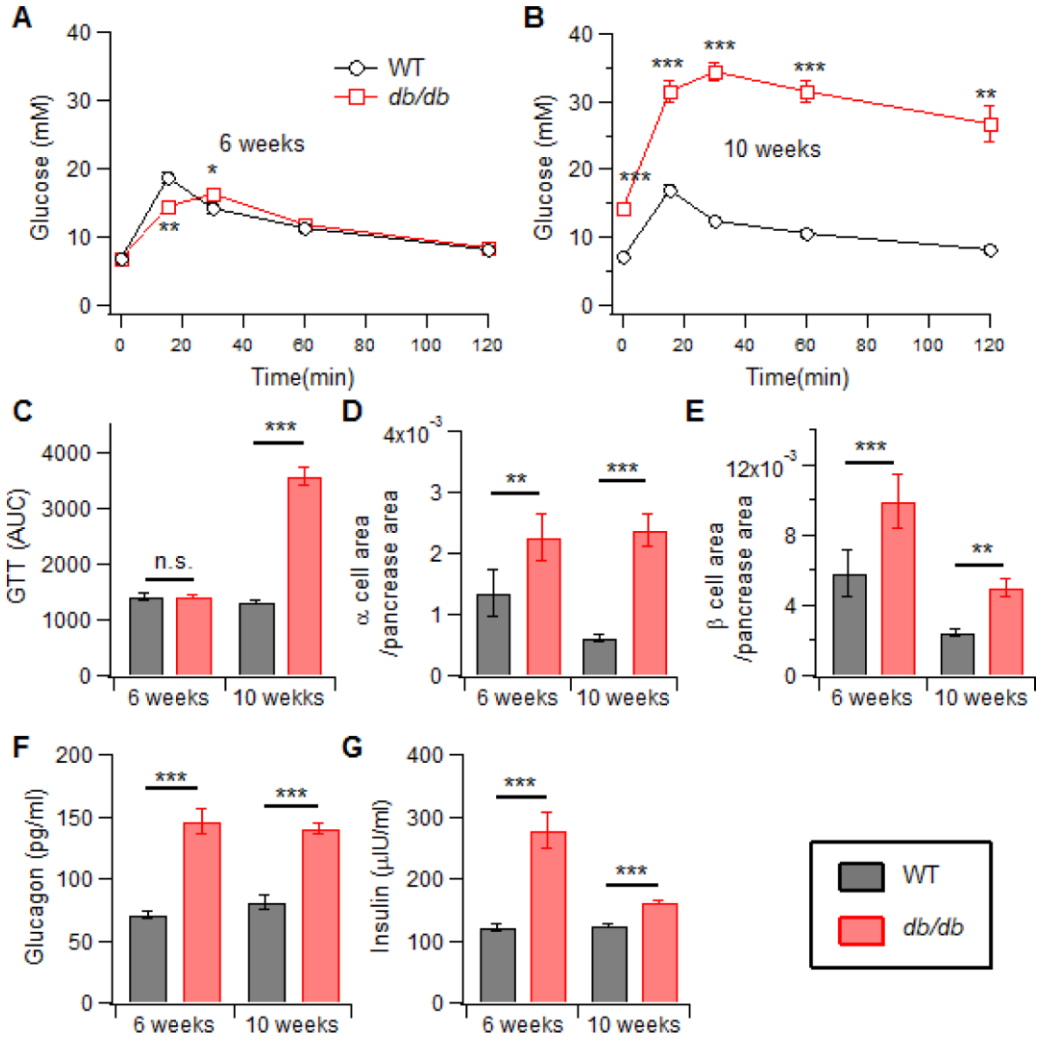

Fig. S3. Changes in the glucose tolerance and α- and β-cell mass and function during diabetes pathogenesis in *db/db* mice. (A, B) IPGTT curves of six- and ten-week-old wild type mice and *db/db* mice (n = 6). **(C)** Area under the curve (AUC) of IPGTT of six- and ten-week-old wild type and *db/db* mice from **(A, B)**. **(D)** The ratio of the α-cell area *versus* the total pancreas area in six- and ten-week-old control and *db/db* mice (n = 6). **(E)** The ratio of the β-cell area *versus* the total pancreas area in six- and ten-week-old control and *db/db* mice (n = 6). **(F)** Glucagon secretion in isolated islets from six- and ten-week-old control and *db/db* mice (n = 6). **(G)** Glucose stimulated insulin secretion in isolated islets from six- and ten-week-old control and *db/db* mice (n = 6).

Journal of Cell Science • Supplementary information

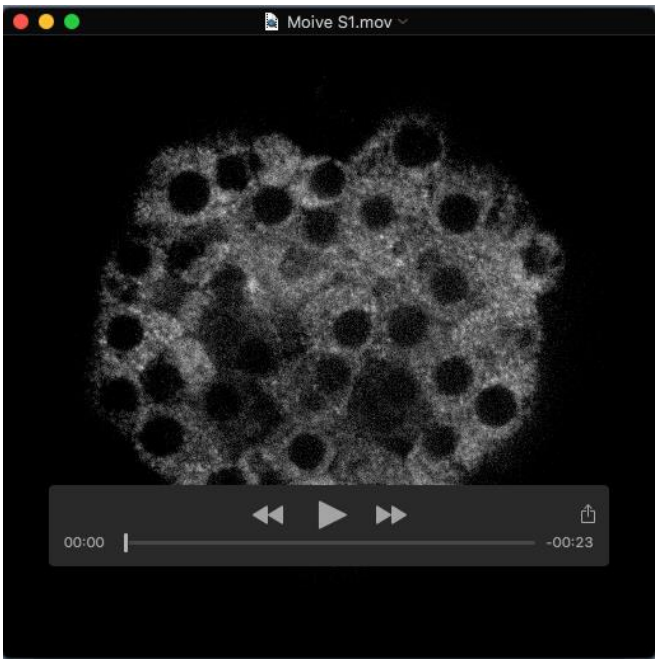

Movie. S1. A representative time-lapse movie of a ZRL1-labeled islet that is sequentially perfused with TPEN and NH_4Cl.

Journal of Cell Science • Supplementary information